Shock Waves (1994) 4:1–10

Shock Waves


# The Sedov self-similar point blast solutions in nonuniform media

D.L. Book

Astronomy Department, University of Maryland, College Park, MD 20742, USA

Received May 11, 1991; accepted in revised form February 9,1994

**Abstract.** The character of a spherical blast wave propagating radially outward in a pressureless medium with density decreasing as $r^{-\omega}$ changes dramatically as $\omega$ and the adiabatic index $\gamma$ vary. Plots of the Sedov formulas for the density, velocity, and pressure profiles behind the shock front for a selection of different parameters illustrate this and suggest that some of the solutions satisfy the conditions for the Rayleigh-Taylor or convective instablity.

**Key words:** Non-uniform media, Point explosion, Self-similar solution

## 1. Introduction

Approximately 50 years ago, von Neumann (1941), Taylor (1941), and Sedov (1946) independently derived a self-similar description of the evolution of the blast wave arising from a powerful explosion in a cold uniform background. They treated the explosion as an instantaneous release of energy at a point and assumed that the background material through which the expanding blast sweeps behaves as an ideal polytropic fluid. It is remarkable that this model yields exact (though algebraically complicated) analytical expressions for the fluid quantities. The form and properties of these solutions were investigated in greatest detail by Sedov and his students. The latter included Korobeĭnikov, who broadened the description (Korobeĭnikov et al. 1961) to background densities given by $\rho_0 = Ar^{-\omega}$, where $A$ and $\omega$ are constants. In the most general formulation of the point blast the distance $R_s$ from the center of symmetry to the shock position is given as a function of time by

$$R_s = \left(\frac{Et^2}{\alpha A}\right)^{\frac{1}{\nu+2-\omega}}, \tag{1}$$

where $E$ is the explosion energy, $\nu = 1, 2, 3$ is the dimensionality of space, and $\alpha$ is a constant depending on $\nu$, $\omega$, and $\gamma$. The density, velocity, and pressure in the region $r \leq R_s$ can be nondimensionalized with respect to their values at the shock and written as

$$\rho(r,t) = \rho_s D(\xi);\ v(r,t) = v_s V(\xi);\ p(r,t) = p_s P(\xi), \tag{2}$$

where

$$\rho_s = \frac{\gamma+1}{\gamma-1}\rho_0;\ v_s = \frac{2\dot{R}_s}{\gamma+1};\ p_s = \frac{2\rho_0 \dot{R}_s^2}{\gamma+1}, \tag{3}$$

$\xi = r/R_s$ is the similarity variable, $\dot{R}_s \equiv \mathrm{d}R_s/\mathrm{d}t = 2R_s/(\nu+2-\omega)t$ is the shock velocity, and the dimensionless fluid variables satisfy

$$D(1) = V(1) = P(1) = 1. \tag{4}$$

The corresponding implosion problem, first studied by Guderley (1942), also gives rise to similarity solutions.

These solutions have been applied to chemical and nuclear explosions (Taylor 1950) and supernova evolution (Chevalier 1976), and have been extended to the study of detonations (Sedov 1959) and expanding laser plasmas (Leonard and Mayer 1975; Ripin et al. 1988). Grigorian (1958) noted two limiting cases for which the front moves according to an exponential or logarithmic law instead of (1). Zel'dovich and Raĭzer (1966) employed the latter to treat blast waves propagating in an exponential atmosphere. Oppenheim and his students (Oppenheim et al. 1972) developed a formalism which unifies the treatment of all cases of blast wave and detonations. Chernyĭ (1957) found a useful approximation to the blast-wave solution in which the profiles are regarded as thin shells surrounding a bubble of uniform pressure and negligible density. This model, which simplifies the algebraic form of the Sedov formulas, is also described by Zel'dovich and Raĭzer (1966). The solutions for the implosion problem have been applied to laser pellet compression (Kidder 1974; 1976) and to the motion of collapsing bubbles (Hunter 1960). Butler (1954) discovered another approximation, applicable to the implosion case. This was elaborated by Whitham (1974) (the so-called Whitham or Chester-Chisnell-Whitham technique).

Until recently very little was known about the linear stability of these solutions. Lifshitz (1946), in studying galaxy

formation in the early expansion of the universe, and Kidder (1976) and Bernstein and Book (1978), in connection with laser pellet implosions, studied non-blast-wave self-similar motions for which the dimensionless velocity $V$ is proportional to $\xi$. These are sometimes called "uniform" or "homogeneous" flows. They found several instances of instability, but blast waves behind which the flow is uniform (which entails a particular relation between $\nu$, $\omega$, and $\gamma$) turn out to be stable (Bernstein and Book 1980). In a series of papers published in the past decade, however, Ryu and Vishniac (1987; 1989) have shown for $\omega = 0$ (uniform background) that the Sedov solutions are unstable when $\gamma$ is sufficently small. Kohlberg and Book (1991) have reached a similar conclusion using the linearized form of the Chernyĭ approximation to study blast wave stability in arbitrarily varying atmospheres.

Sedov's book, which has gone through ten Russian editions and three English translations, is the bible of the subject of self-similarity in fluid mechanics. But like the Bible, it has been more reverenced (and referenced) than read. Perhaps this partly reflects the uncongeniality of the formalism used to solve the equations. The variables that are mathematically most convenient (the dimensionless velocity and the square of the dimensionless sound speed) do not lend themselves readily to physical interpretation. Practitioners who are adept at manipulating these quantities tend to present their results in the form of phase diagrams, instead of the more transparent plots of density, velocity, and pressure against $\xi$.

Whatever the reason, there are indications (see below) that no one has ever used the formulas of Sedov and Korobeĭnikov to plot out $D$, $V$, and $P$ as functions of $\xi$ for a representative selection from the entire parameter space ($\nu$, $\omega$, and $\gamma$) in order to exhibit their behavior systematically. The only instances in the literature appear to be treatments of particular cases, e.g., the survey of the profiles for $\omega = 0$ as a function of $\gamma$ by Sakurai (1953) for $\nu = 1$, 2 and by Sedov (1959) for $\nu = 3$, and for $\nu = 3$ and $\gamma = 4/3$ as a function of $\omega$ by Chevalier (1976). The present paper describes calculations I have undertaken with the aim of repairing this deficiency and making the results readily available to the community. I have calculated and plotted the physical profiles for $\gamma = 1.1$, 1.2, 1.3, 1.4, 1.5, and $5/3$ (the values appropriate to ordinary gases) and $0 \leq \omega < 3$ (the values for which the total mass in the region $r < R_s$ is finite) for $\nu = 3$. To keep the number of figures within reasonable bounds, I have not carried out a similarly complete survey for $\nu = 1$ and 2, but include a few examples in order to indicate how they differ. I have concentrated on spherical explosions ($\nu = 3$) because they are the most interesting for the majority of applications; in any event, the dependence on $\nu$ is weaker than for the other two parameters.

The shapes of the profiles revealed by this survey are considerably more diverse than I would have guessed. They vary most rapidly for small values of $\gamma$ and large values of $\omega$. In addition to confirming the morphological description provided by Sedov (1959) and Korobeĭnikov et al. (1961), I found several new features. As noted by Chevalier (1976) for $\gamma = 4/3$, in a certain interval of the parameters $\rho$ decreases as a function of radius just behind the front while $p$ is decreasing. In other words, the gradients of density and pressure have opposite sign—the signature of the presence of Rayleigh-Taylor instability. Repeating these plots using slightly different values of $\omega$ and $\gamma$ yields a picture of how sensitively this characteristic depends on these parameters. But even when Rayleigh-Taylor instability is absent, there are indications that many of these states are subject to convective instability. In other words, they behave as if a cold region is supported from below against gravity by a warmer one. The criterion for this is that the quantity $p\rho^{-\gamma}$ (the exponential of the entropy) decrease "upward," i.e., in the direction in which $p$ decreases (Landau and Lifshitz 1987; Book 1979).

A by-product of the exercise was the discovery that there is a sign error in the argument of the exponential in Eqs. (2.73) and (2.74) of Korobeĭnikov et al. (1961). This could be just a misprint, but it has been reproduced unchanged—and apparently unchecked—in every subsequent edition of Sedov's book through the tenth (1987).

Some people (specifically, the adepts referred to above) will prefer to generate these profiles by integrating the differential equations numerically. Certainly this is more elegant, and even requires fewer computational operations. But numerical integration necessitates an excursion into Sedov's fearsome phase space and an understanding of the somewhat exotic subject of classification of singularities of ordinary differential equations, whereas plugging numbers into the formulas is almost completely trivial. Besides, if the Sedov formulas are not meant to be plotted, then what are they good for?

Section 2 summarizes the relations used to produce the plots, taken from Korobeĭnikov et al. (1961) (For the most part I have followed their notation, but instead of their $f$, $g$, and $h$, I have written $D$, $V$, and $P$ respectively, which are more mnemonic. There are also a few other minor changes). Section 3 consists of two tables and 104 plots. Each figure except the last two contains multiple frames displaying plots of $D$, $V$, and $P$ vs. $\xi$ for a particular choice of $\nu$, $\omega$, and $\gamma$. The last figure displays numerical values of the normalization constant $\alpha$, an analytic expression for which is known only in the case of uniform self-similarity, for a matrix of values of $\omega$ and $\gamma$. The tables are guides to the figures. They show which of the cases in the matrix are plotted and where. I conclude with a brief discussion of these results in Sect. 4, touching on the subjects of Rayleigh-Taylor and convective instability. An appendix describes the program written in Fortran 77 which I used to generate them.

## 2. The Sedov formulas for variable background density

When the one-dimensional ideal fluid equations

$$\frac{\partial \rho}{\partial t} + \frac{1}{r^{\nu-1}} \frac{\partial (r^{\nu-1} \rho v)}{\partial r} = 0; \tag{5}$$

$$\frac{\partial v}{\partial t} + v \frac{\partial v}{\partial r} + \frac{1}{\rho} \frac{\partial p}{\partial r} = 0; \tag{6}$$

$$\frac{\partial (p\rho^{-\gamma})}{\partial t} + v \frac{\partial (p\rho^{-\gamma})}{\partial r} = 0, \tag{7}$$

are nondimensionalized according to (2) and solved subject to (4), the results can be written parametrically in terms of a quantity $F$ (Korobeĭnikov et al. 1961):

$$\xi = F^{-\beta_6}\,[C_1\,(F - C_2)]^{\beta_2}\,[C_3\,(C_4 - F)]^{-\beta_1}\,; \tag{8}$$

$$D = F^{\beta_7}\,[C_1\,(F - C_2)]^{\beta_3 - \omega\beta_2}\,[C_3\,(C_4 - F)]^{\beta_4 + \omega\beta_1} \times [C_5\,(C_6 - F)]^{-\beta_5}\,; \tag{9}$$

$$V = \xi F; \tag{10}$$

$$P = F^{\beta_8}\,[C_3\,(C_4 - F)]^{\beta_4 + (\omega - 2)\beta_1} \times [C_5\,(C_6 - F)]^{1 - \beta_5}\,, \tag{11}$$

where

$$\begin{aligned} &\beta_0 = \frac{1}{\nu\gamma - \nu + 2};\ \beta_1 = \beta_2 + (\gamma + 1)\beta_0 - \beta_6; \\ &\beta_2 = \frac{\gamma - 1}{\gamma(\omega_2 - \omega)};\ \beta_3 = \frac{\nu - \omega}{\gamma(\omega_2 - \omega)}; \\ &\beta_4 = \beta_1\frac{(\nu - \omega)(\nu + 2 - \omega)}{\omega_3 - \omega};\ \beta_5 = \frac{2\nu - \omega(\gamma + 1)}{\omega_3 - \omega}; \\ &\beta_6 = \frac{2}{\nu + 2 - \omega};\ \beta_7 = \omega\beta_6;\ \beta_8 = \nu\beta_6, \end{aligned} \tag{12}$$

and

$$\begin{aligned} &C_0 = \frac{2^\nu \pi^{\frac{\nu - 1}{2}}\,\Gamma\left(\frac{\nu + 1}{2}\right)}{\Gamma(\nu)};\ C_1 = \gamma C_5;\ C_2 = \frac{C_6}{\gamma}; \\ &C_3 = \frac{\nu\gamma - \nu + 2}{(\omega_1 - \omega)C_6};\ C_4 = (\nu + 2 - \omega)\beta_0 C_6; \\ &C_5 = \frac{2}{\gamma - 1};\ C_6 = \frac{\gamma + 1}{2}, \end{aligned} \tag{13}$$

with

$$\begin{aligned} &\omega_1 = \frac{3\nu - 2 + \gamma(2 - \nu)}{\gamma + 1};\ \omega_2 = \frac{2(\gamma - 1) + \nu}{\gamma}; \\ &\omega_3 = \nu(2 - \gamma). \end{aligned} \tag{14}$$

[In place of $C_0$ Sedov uses $2(\nu - 1)\pi + (\nu - 2)(\nu - 3)$, a simple interpolation which reduces to the correct values for $\nu = 1$, 2, and 3, but is formally incorrect.]

For $\nu = 3$ (14) imply

$$\omega_3 \le \omega_1 \le \omega_2, \tag{15}$$

with equality only for $\gamma = 1$. For $\omega < \omega_1$ the parameter $F$ goes from $C_2$ to 1 as $\xi$ varies from 0 to 1. For $\omega > \omega_1$ it varies from $C_6$ to 1 as $\xi$ goes from a value $\xi_0 > 0$ to 1; the region $0 \le \xi < \xi_0$ is a "hole" within which the density and pressure vanish. When $\xi$ approaches $\xi_0$ from the right the density diverges in the cases $\omega_4 < \omega < \omega_1$ and $\omega > \max[\omega_1, \omega_5]$, and vanishes otherwise, where

$$\omega_4 = \frac{\nu}{\gamma};\ \omega_5 = \frac{2\nu}{\gamma + 1}. \tag{16}$$

Although the scaled fluid equations (the ordinary differential equations satisfied by $D$, $V$, and $P$ as functions of $\xi$) are analytic in $\nu$, $\omega$, and $\gamma$, Eqs. (8)–(11) appear to become singular for $\omega = \omega_1$, $\omega_2$, or $\omega_3$. These "singularities" are only apparent; they are a consequence of the way the solution is written. Correct forms of $D$, $V$, and $P$ for these cases can be found directly or by taking the limits $\omega \to \omega_j$, $j = 1, 2, 3$. The results are as follows:

For $\omega = \omega_1$,

$$D = \xi^{\nu - 2}; \tag{17}$$

$$V = \xi; \tag{18}$$

$$P = \xi^\nu. \tag{19}$$

(This is the uniform self-similar case, mentioned in Sect. 1.)

For $\omega = \omega_2$,

$$\xi = F^{-\beta_6}\,[C_1\,(F - C_2)]^{(\gamma - 1)\beta_0} \times \exp\left[\frac{(\gamma + 1)\beta_0(1 - F)}{F - C_2}\right]; \tag{20}$$

$$D = F^{\beta_7}\,[C_1\,(F - C_2)]^{(4 - \nu - 2\gamma)\beta_0}\,[C_5\,(C_6 - F)]^{-\beta_5} \times \exp\left[\frac{-2(\gamma + 1)\beta_0(1 - F)}{F - C_2}\right]; \tag{21}$$

$$P = F^{\beta_8}\,[C_1\,(F - C_2)]^{-\nu\gamma\beta_0}\,[C_5\,(C_6 - F)]^{1 - \beta_5}\,. \tag{22}$$

Here (and in the next case) $V$ is given by (10). As noted in the Introduction, the sign in the argument of the exponential of (20) and (21) differs from that given by Sedov (1959) and Korobeĭnikov et al. (1961). For $\omega = \omega_3$,

$$\xi = F^{-\beta_6}\,[C_1\,(F - C_2)]^{\beta_2}\,[C_5\,(C_6 - F)]^{-\beta_1}\,; \tag{23}$$

$$D = F^{\beta_7}\,[C_1\,(F - C_2)]^{\beta_3 - \omega\beta_2}\,[C_5\,(C_6 - F)]^{1 - 4\beta_0} \times \exp\left[\frac{-\nu\gamma(\gamma + 1)\beta_0\,(1 - F)}{C_6 - F}\right]; \tag{24}$$

$$P = F^{\beta_8}\,[C_5\,(C_6 - F)]^{2(\nu\gamma - \nu - \gamma)\beta_0} \times \exp\left[\frac{-\nu\gamma(\gamma + 1)\beta_0\,(1 - F)}{C_6 - F}\right]. \tag{25}$$

The constant $\alpha$ that appears in (1) is given by

$$\alpha = \frac{8C_0}{(\gamma^2 - 1)(\nu + 2 - \omega)^2}\int_0^1 \xi^{\nu - 1}\left(DV^2 + P\right)\mathrm{d}\xi. \tag{26}$$

The quadrature must be carried out numerically except for the case $\omega = \omega_1$, which can be evaluated in closed form to give

$$\alpha = \frac{2C_0(\gamma + 1)}{\nu(\gamma - 1)(\nu\gamma - \nu + 2)^2}. \tag{27}$$

## 3. Results

For $\nu = 1$ (Fig. 1) I have calculated and plotted $D$, $V$, and $P$ only for $\gamma = 1.1$ and $\gamma = 5/3$. Here and in what follows, density is indicated by a solid line, velocity by long dashes, and pressure by short dashes. Figure 1a–h displays the results obtained for $\gamma = 1.1$ using eight different values of $\omega$. These were chosen so that there are no drastic changes in behavior from one case to the next, i.e., they are roughly evenly separated in "phenomenology space." It is noteworthy that this causes most values of $\omega$ to be crammed into the uppermost ten percent of the range [0, 1].

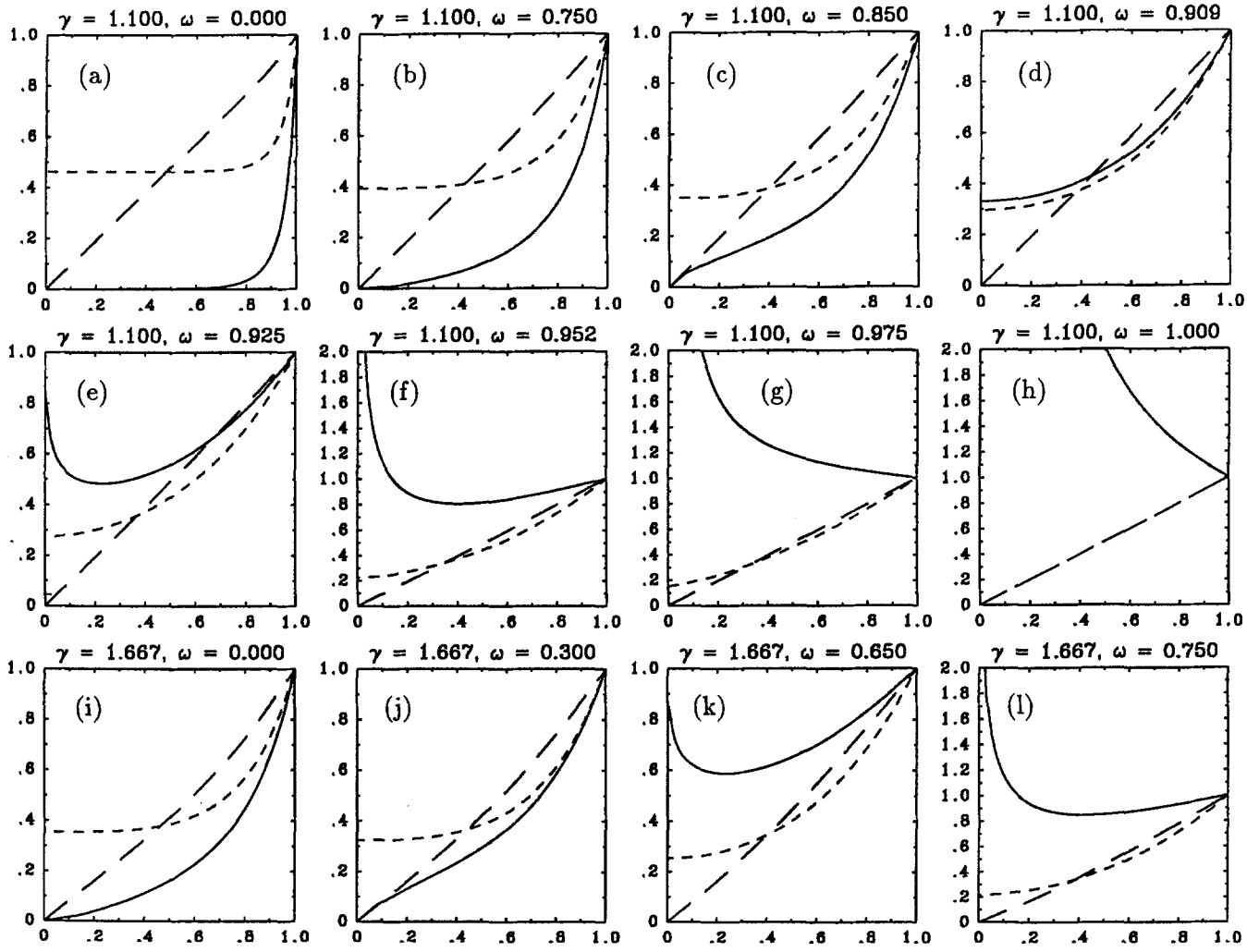


**Fig. 1.** Plots of $D$, $V$, and $P$ (solid trace, long dashes, and short dashes, respectively) vs. scaled radius $\xi$ for $\nu = 1$ with $\gamma$ and $\omega$ as shown

(Throughout this paper I have restricted myself to $0 \leq \omega < \nu$, thus satisfying the requirement that the mass swept over by the blast wave in the region $0 \leq r \leq R_s$ be finite.) These cases include $\omega = \omega_1$, $\omega_4$, and $\omega_5$. Nothing very interesting happens at $\omega_3$; $\omega_2$ is outside the allowed range.

When $\omega$ varies from 0 to 1 the following qualitative changes occur: (i) The density develops an inflection point (Fig. 1c) and then (ii) becomes non-zero at $\omega = \omega_4$ (Fig. 1d). (iii) For $\omega > \omega_4$ the density diverges at the origin. (iv) As $\omega \rightarrow \omega_1$ (Fig. 1h) the pressure goes to zero at the origin. Exactly the same behavior takes place for $\gamma = 5/3$ (Fig. 1i–l), but each stage is observed at a smaller $\omega$, so that the action is spread out over the whole range of $\omega$. For $\nu = 1$ the value of $\omega_1$ is unity for all values of $\gamma$. Moreover, as (17)–(19) show, $D$, $V$, and $P$ depend only on $\nu$. Thus for $\nu = \omega = 1$ Fig. 1h also gives the correct profiles for $\gamma = 5/3$ or any other value of $\gamma$, and $V$ and $P$ coincide.

Figure 2a–h displays analogous results for $\nu = 2$ and $\gamma = 1.1$ with $\omega$ between 0 and 2. Now $\omega_2 = 2$ holds, independent of $\gamma$, and a new phenomenon occurs for $\omega_1 < \omega \leq \omega_2$: (v) a hole develops in a neighborhood of the origin, within which the density and pressure vanish. The velocity is finite at the hole boundary. As $\omega$ continues to increase the pressure, initially concave upward, becomes (vi) convex and then in the limit $\omega \rightarrow \omega_2$ (vii) discontinuous at the boundary of the hole. The same stages occur for $\gamma = 5/3$ (Fig. 2i–p); as with $\nu = 1$, they are spread out over a broader range of $\omega$.

For $\nu = 3$, three qualitatively new developments occur: (viii) when the hole at the origin develops, the density is convex upward; (ix) it bulges upward more and more with increasing $\omega$, eventually developing a local maximum; and (x) as $\omega \rightarrow \omega_5$ it becomes discontinuous at the periphery of the hole and divergent thereafter. These same ten stages occur in the same order for all values of $\gamma$ with $\nu = 3$; only the values of $\omega$ marking the locations of the transitions change. The slope of $D$ is negative for $\omega$ sufficiently large.

Figure 6a and 6b displays the profiles for $\omega = \omega_1$ in the two- and three-dimensional cases, respectively. As noted above in connection with $\nu = 1$, there is no dependence on $\gamma$. (Two traces appear to be missing: for $\nu = 2$ the density profile equals unity and coincides with the upper border of the frame, while for $\nu = 3$ the density and velocity profiles are identical.) The "entropy" (actually, $S = PD^{-\gamma}$, which is linearly related to the exponential of the specific entropy) for $\gamma = 1.1$ and $\gamma = 5/3$ is plotted in Fig. 6c and 6d respectively, for ten different values of $\omega$. Finally, Fig. 7

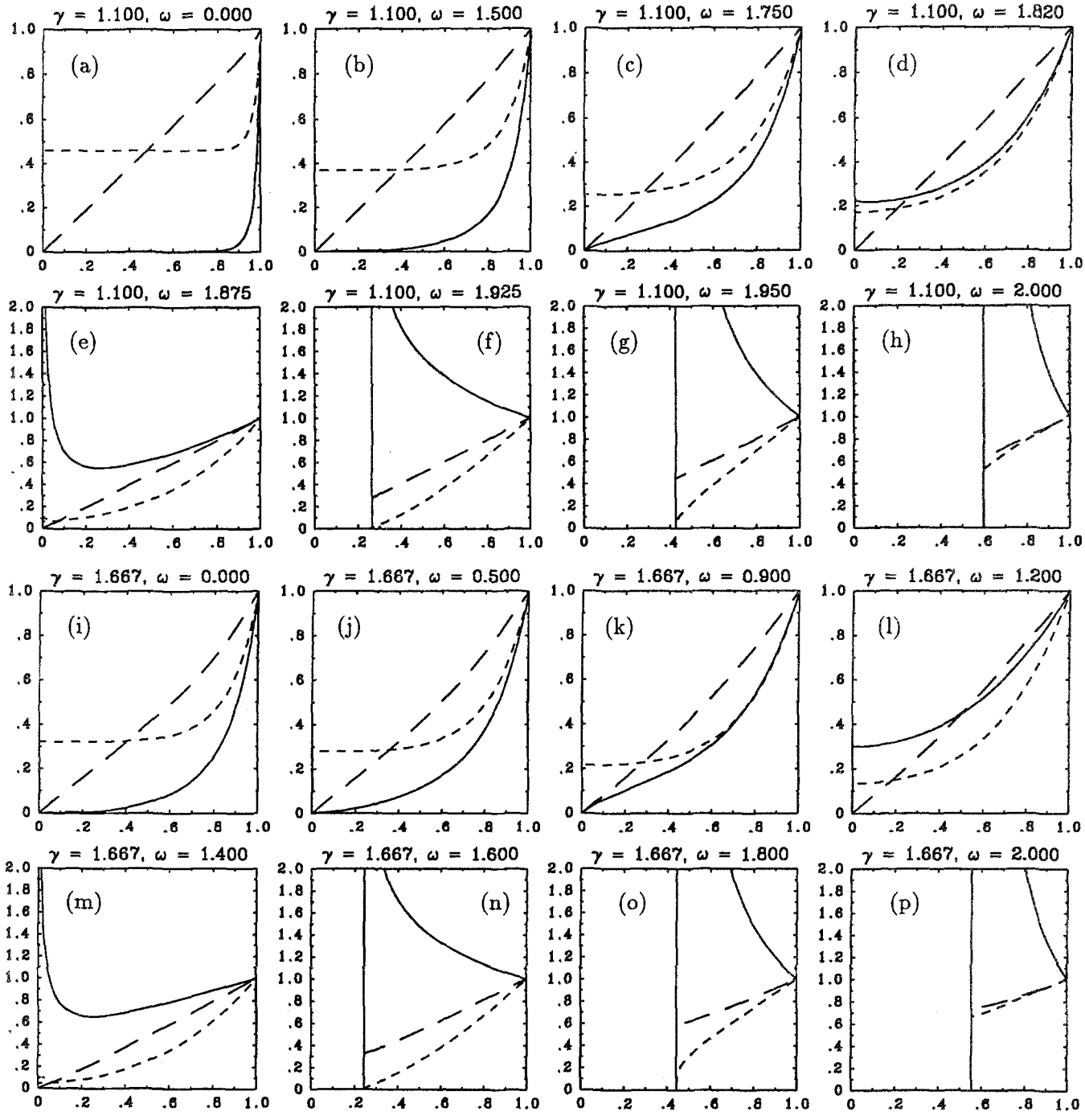


**Fig. 2.** Plots of $D$, $V$, and $P$ (solid trace, long dashes, and short dashes, respectively) vs. scaled radius $\xi$ for $\nu = 2$ with $\gamma$ and $\omega$ as shown

displays the normalization constant $\alpha$ for the various values $\gamma$ as a function of $\omega$ for $\nu = 3$, obtained by numerical integration of (26).

## 4. Discussion

I performed the above calculations in connection with research on the stability of blast waves in a variable atmosphere (Kohlberg and Book 1991). My motivation was to find out whether the profiles of the Sedov solutions could be nonmonotonic as functions of $\xi$. As this ultimately turned out to involve a fair amount of work, I resolved to share the information with others who might find it useful. The problem was to select from all possible cases enough to display all the typical features and to reveal the effect of varying just one parameter at a time, and to do this in a reasonably concise manner. These requirements are inconsistent. When $\gamma$ is large, displaying the full range of behavior necessitates plotting cases with $\omega$ spread over most of the allowable range $[0, \nu]$. When $\gamma$ is small the profiles for the same values of $\omega$ show very little variation, because everything happens in a narrow range of $\omega$ close to $\nu$.

In order to escape from this box, I have taken the view that comparisons should be made between adjacent

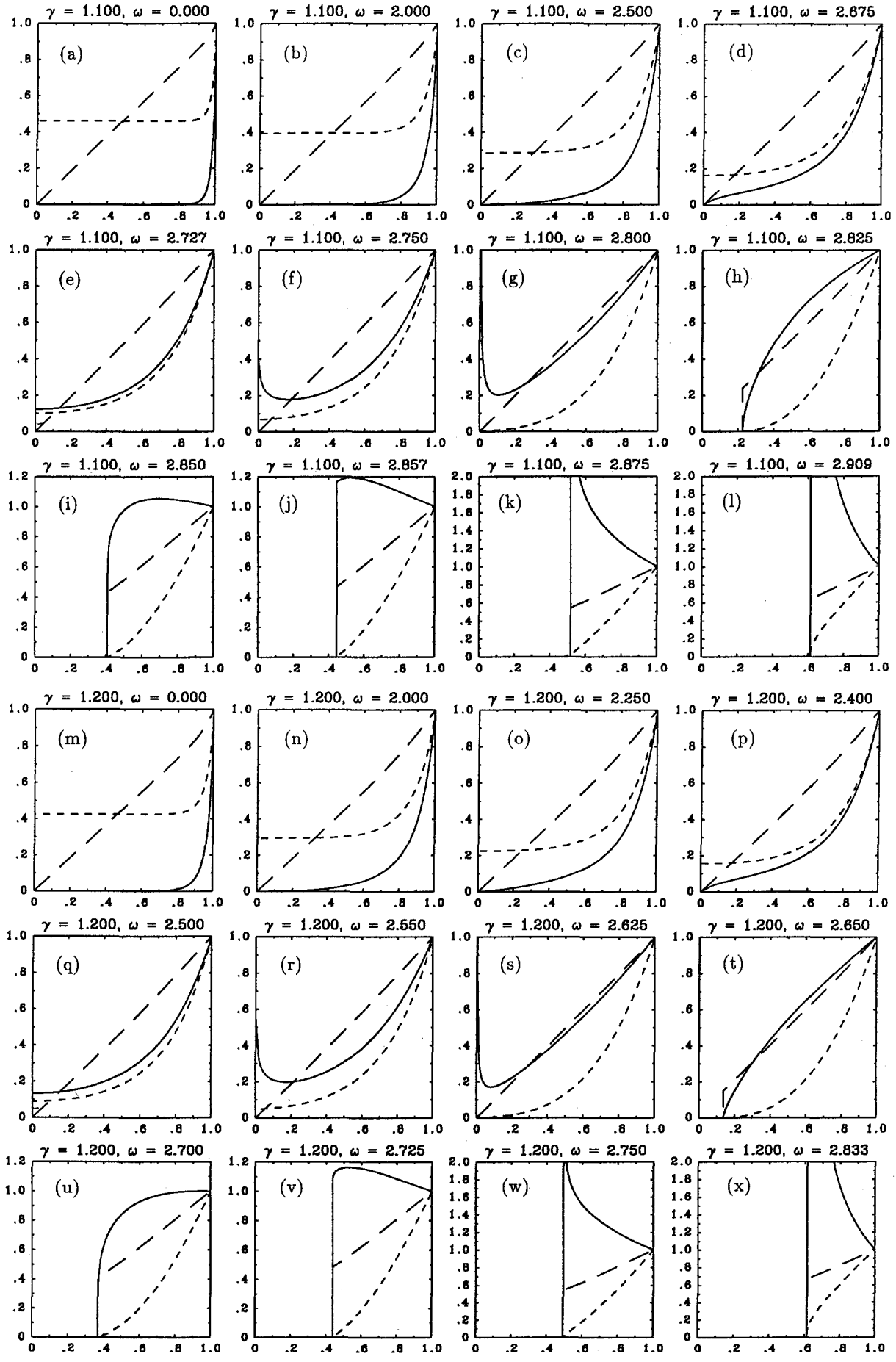


**Fig. 3.** Plots of $D$, $V$, and $P$ (solid trace, long dashes, and short dashes, respectively) vs. scaled radius $\xi$ for $\nu = 3$ with $\gamma$ and $\omega$ as shown

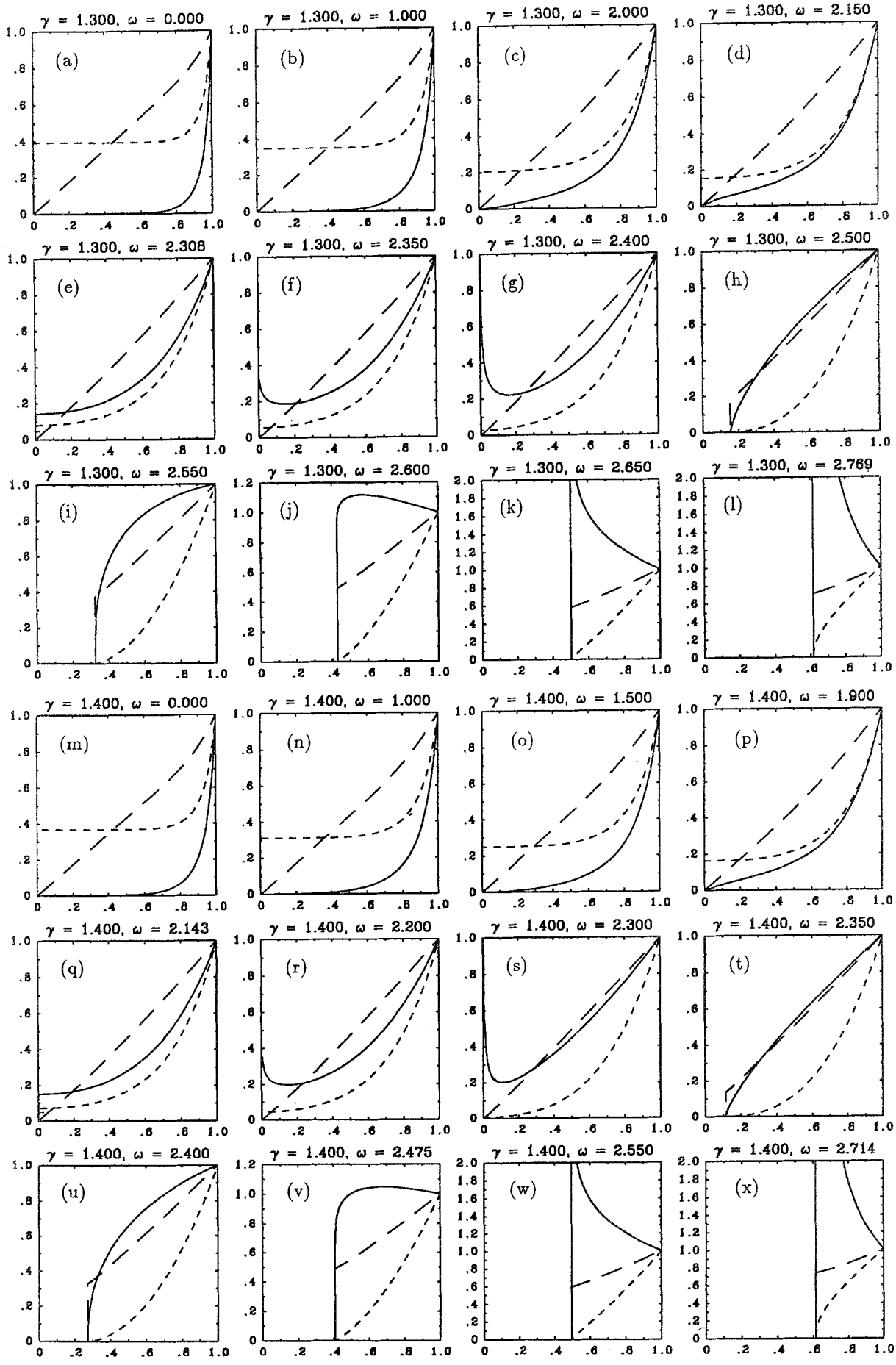


**Fig. 4.** Plots of $D$, $V$, and $P$ (solid trace, long dashes, and short dashes, respectively) vs. scaled radius $\xi$ for $\nu = 3$ with $\gamma$ and $\omega$ as shown

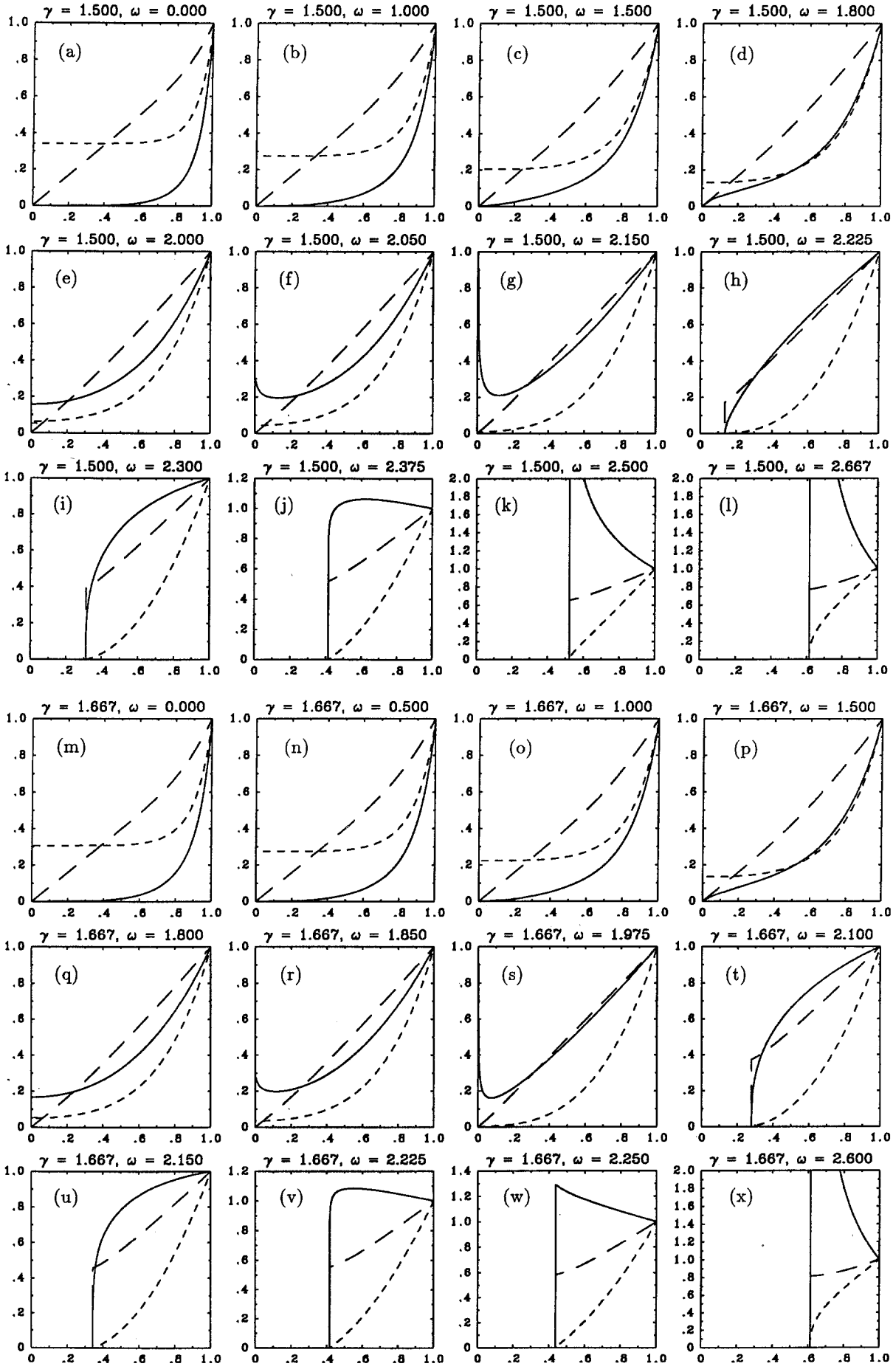


**Fig. 5.** Plots of $D$, $V$, and $P$ (solid trace, long dashes, and short dashes, respectively) vs. scaled radius $\xi$ for $\nu = 3$ with $\gamma$ and $\omega$ as shown

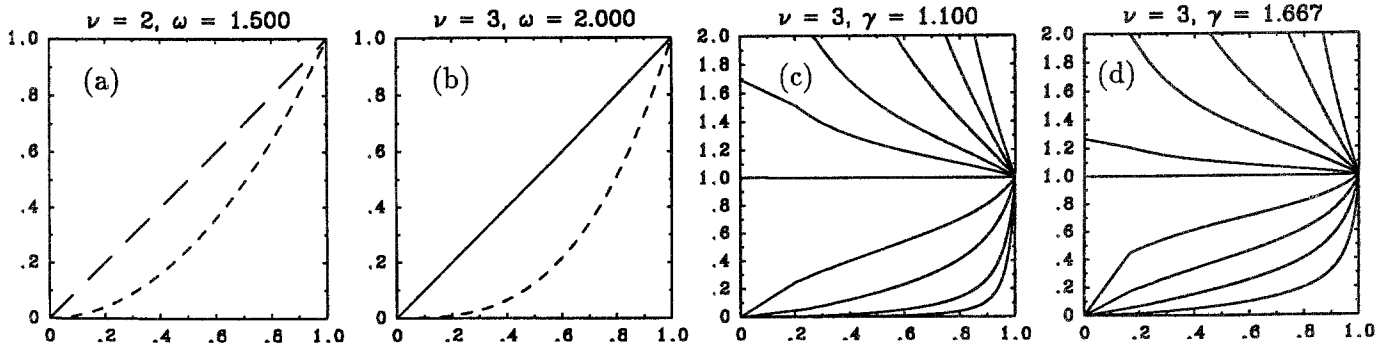


**Fig. 6.** Plots of $D$, $V$, and $P$ (solid trace, long dashes, and short dashes, respectively) vs. scaled radius $\xi$ at $\omega = \omega_1$ for arbitrary $\gamma$ and (a) $\nu = 2$, (b) $\nu = 3$; plots of entropy $S = PD^{-\gamma}$ with $\nu = 3$ and (c) $\gamma = 1.1$, for $\omega = 2.5$, 2.65, 2.69, 2.71, 2.72, 2.72727, 2.75, 2.77, 2.79, and 2.83 (top to bottom), and (d) $\gamma = 5/3$, for $\omega = 1.0$, 1.6, 1.72, 1.76, 1.79, 1.8, 1.84, 1.88, 1.92, and 1.96 (top to bottom)

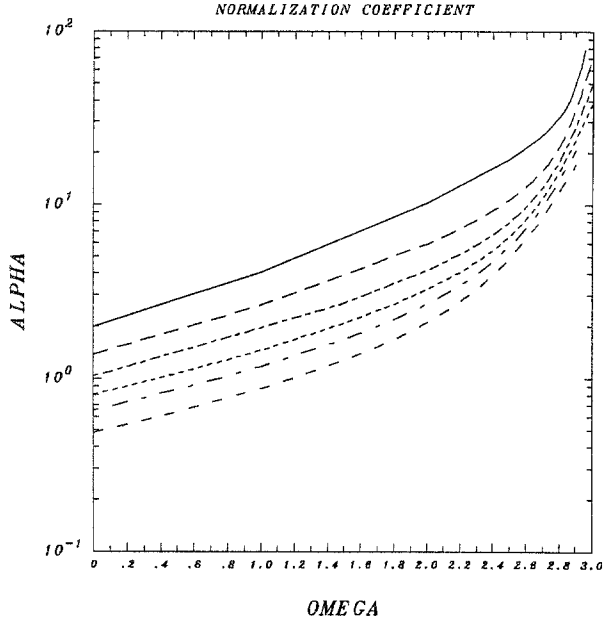


**Fig. 7.** Plots of $\alpha$ as a function of $\omega$ for $\gamma = 1.1$, 1.2, 1.3, 1.4, 1.5, and 5/3, respectively, reading from top to bottom

**Table 1.** Locator for $\nu = 1$ and $\nu = 2$ plots

| Stage | $\nu = 1$ | | $\nu = 2$ | |
|---|---|---|---|---|
| | $\gamma = 1.1$ | $\gamma = 5/3$ | $\gamma = 1.1$ | $\gamma = 5/3$ |
| $\omega = 0$ | 1a | 1i | 2a | 2i |
| (i) | 1c | 1j | 2c | 2k |
| $\omega = \omega_4$ | 1d | 1k | 2d | 2l |
| (iii) | 1e | 1l | 2e | 2m |
| (v) | — | — | 2f | 2n |
| $\omega = \omega_1$ | 1h | 1h | 6a | 6a |
| $\omega = \omega_5$ | 1g | 1l | 6a | 6a |
| $\omega = \omega_2$ | — | — | 2h | 2p |

**Table 2.** Locator for $\nu = 3$ plots. Figure numbers in parentheses are for $\omega$ close to but not exactly coincident with $\omega_5$

| Stage | $\gamma$ | | | | | |
|---|---|---|---|---|---|---|
| | 1.1 | 1.2 | 1.3 | 1.4 | 1.5 | 5/3 |
| $\omega = 0$ | 3a | 3m | 4a | 4m | 5a | 5m |
| (i) | 3d | 3p | 4d | 4p | 5d | 5p |
| $\omega = \omega_4$ | 3e | 3q | 4e | 4q | 5e | 5q |
| (iii) | 3f | 3r | 4f | 4r | 5f | 5r |
| $\omega = \omega_1$ | 6b | 6b | 6b | 6b | 6b | 6b |
| (viii) | 3h | 3t | 4h | 4t | 5h | 5t |
| (ix) | 3i | 3v | 4j | 4v | 5j | 5v |
| $\omega = \omega_5$ | 3j | (3v) | (4j) | (4v) | (5j) | (5v) |
| $\omega = \omega_2$ | 3l | 3x | 4l | 4x | 5l | 5x |

points in "phenomenology space." That is, I have presented cases for different $\gamma$ at the same special $\omega_j$ [defined as functions of $\gamma$ through (14) and (16)] and at more or less equivalent intermediate points. Tables 1 and 2 are intended to facilitate this comparison process. It is evident that, except for $\omega = \omega_1$, phenomenologically equivalent cases are not identical, although for the most part they are very close.

Of the three dependent variables, $V$ varies the least and $D$ the most as a function of the parameters $\nu$, $\gamma$, and $\omega$. In fact, in all cases $V$ is nearly linear with radius, and when no hole is present it is well approximated by $V = \xi$. As noted above, for all $\gamma$ and $\nu$ there are ranges of $\omega$ within which $D$ has negative slope over some or all of the range of $\xi$. Since the slope of $P$ is always positive (which means that the direction of decreasing $\xi$ is "up"), the two have opposite signs. Hence these regions are formally Rayleigh-Taylor-unstable, and an instability will develop that tends to overturn or interchange material of high and low density. A rigorous calculation of the growth of even small-amplitude perturbations seems out of the question. The task is complicated not only by the space- and time dependence of the basic state, but by the difficulty of obtaining the correct boundary conditions at the shock front, which is continually sweeping over new material. The problem is analogous to that of calculating the stability of a detonation front or an ablating pellet (Bodner 1974; Takabe et al. 1985). Nevertheless, it seems likely that at sufficiently short wavelengths, for which the growth is likely to be fastest, the behavior will resemble that of the classical Rayleigh-Taylor instability.

Previous workers seem to have overlooked the possibility of a second fluid interchange instability, the convective mode. The criterion for the onset of convective interchange in static media (Landau and Lifshitz 1987) is that $p\rho^{-\gamma}$ be decreasing upward, i.e., $\mathrm{d}S/\mathrm{d}\xi > 0$. Elsewhere (Book 1979) I have shown that the same criterion holds in the case of uniform self-similar expansion. The generalization to arbitrary self-similar flows does not quite work; the derivation fails because the acceleration varies as a function of the scaled radius. Since this variation is extremely weak, however, the same criterion probably applies except close to $S' = 0$. Evidently (Fig. 6c, 6d) it can be satisfied even if $D' > 0$. In fact, as pointed out by Korobeĭnikov et al. (1961), $S' > 0$ holds for all $\omega > \omega_4$.

## Appendix

### A program for plotting the fluid variables

It is straightforward to write a program to calculate $D(\xi)$, $V(\xi)$, and $P(\xi)$ by substituting successive values of $F$ in (8)–(11). The only nontrivial part is figuring out how to handle the cases $\omega \approx \omega_j$, $j = 1, 2, 3$. While the results given in (16)–(26) can be obtained analytically as limiting forms of the general case, numerically when $\omega$ is close to $\omega_j$ two bad things happen: some of the exponents become very large, creating overflows, and the spacing between successive values of $\xi$ becomes large near $\xi_0$, making the plots irregular there. I have therefore coded the "singular" formulas separately and inserted tests and branches to the various special cases. The minimum allowable deviation between $\omega$ and $\omega_j$ (called `TEST` in the code) depends on the computer architecture and the number of points in the plot and therefore has to be set by hand. The plot routine, which is likewise application- and implementation-dependent, has also been left unspecified.

Anybody who wants a copy of the calling sequence can get one by sending an e-mail message to `book@avl.umd.edu`.

*Acknowledgement.* I am indebted to Dr. Ira Kohlberg for originally suggesting, in the course of our investigation of blast-wave stability, that I plot some of the Sedov solutions to see what they look like. This work was supported by the U.S. Naval Research Laboratory, and was prepared for publication with support from ARPA under contract No. F30602 3C0164.

## References

Bernstein IB, Book DL (1978) Rayleigh-Taylor instability of a self-similar spherical expansion. Astrophys J 225:633

Bernstein IB, Book DL (1980) Stability of the Primakoff-Sedov blast wave and its generalizations. Astrophys J 240:223

Bodner SE (1974) Rayleigh-Taylor instability and laser pellet fusion. Phys Rev Lett 33:761

Book DL (1979) Convective instability of self-similar expansion into vacuum. J Fluid Mech 95:779

Butler DS (1954) Converging spherical and cylindrical shocks. Rept No 54/54, Armament Research and Development Establishment, Ministry of Supply, Ft. Halstead, Kent

Chernyĭ GG (1957) The problem of a point explosion. Dokl Akad Nauk SSSR 112:213

Chevalier RA (1976) The hydrodynamics of type II supernovae. Astrophys J 207:872

Grigorian SS (1958) Limiting self-similar one-dimensional nonsteady motion of a gas (Cauchy's problem and the piston problem). J Appl Math Mech 22:187

Guderley G (1942) Starke Kugelige und zylindrische Verdichtungsstösse in der Nähe des Kugelmittelpunktes bzw. der Zylinderachse Luftfahrtforschung 19:302

Hunter C (1960) On the collapse of an empty cavity in water. J Fluid Mech 8:241

Kidder RE (1974) Theory of homogeneous isentropic compression and its application to laser fusion. Nucl Fusion 14:53

Kidder RE (1976) Laser-driven compression of hollow shells: power requirements and stability limitations. Nucl Fusion 16:3

Kohlberg I, Book DL (1991) Use of the thin-shell model to analyze stability of spherical blast waves in a medium of variable ambient density. In: Takayama K (ed) Proc 18th Inter Symp Shock Waves, Springer-Verlag, Berlin

Korobeĭnikov VP, Mel'nikova NS, Ryazanov YeV (1961) Teoriya Tochechnogo Vzryva. FizMatLit, Leningrad. [Transl. (1962) The theory of point explosion. JPRS 14, 334, U.S. Dept. of Commerce, Washington, DC], Chap. 2

Landau LD, Lifshitz EM (1987) Fluid Mechanics, 2nd ed. Pergamon, Oxford, Chap. 1

Leonard TA, Mayer FJ (1975) Helium blast-wave measurements of laser heated microshell targets. J Appl Phys 46:3562

Lifshitz E (1946) On the gravitational instability of the expanding universe. J Phys (USSR) 10:116

von Neumann J (1941) The point source solution. NDRC Division B Rept AM-9. Reprinted in (1963) Taub AH (ed) John von Neumann collected works. Pergamon, Oxford, pp 219–237

Oppenheim AK, Kuhl AL, Lundstrom EA, Kamel MM (1972) A parametric study of self-similar blast waves. J Fluid Mech 52:657

Ripin BH, Grun J, Lee TN, Manka CK, Mclean EA, Mostovych AN, Pawley C, Peyser TA, Stamper JA (1988) Structuring processes in expanding laser-produced plasmas. In: Hora H, Miley GH (eds) Laser interaction and related plasma phenomena, Vol. 8. pp 417–433

Ryu D, Vishniac ET (1987) The growth of linear perturbations of adiabatic shock waves. Astrophys J 313:820

Sakurai A (1953) On the propagation and structure of a blast wave: I. J Phys Soc Jpn 8:662

Sedov LI (1946) The movement of air in a strong explosion. Dokl Akad Nauk SSSR 52:17

Sedov LI (1959) Similarity and dimensional methods in mechanics. Academic Press, New York, Chap. 4

Takabe H, Mima K, Montierth L, Morse RL (1985) Self-consistent growth rate of the Rayleigh-Taylor instability in an ablatively accelerating plasma. Phys Fluids 28:3676

Taylor GI (1941) The formation of a blast wave by a very intense explosion. Brit Rept RC-210. Reprinted in (1950) Proc Roy Soc A 186:159

Vishniac ET, Ryu D (1989) On the stability of decelerating shocks. Astrophys J 337:917

Whitham GB (1974) Linear and nonlinear waves. Wiley, New York, Chap. 8

Zel'dovich YaB, Raĭzer YuP (1966) Physics of shock waves and high-temperature hydrodynamic phenomena, vol. I. Academic Press, New York, Chap. 1

This article was processed using Springer-Verlag TEX Shock Waves macro package 1.0 and the AMS fonts, developed by the American Mathematical Society.